

AperTO - Archivio Istituzionale Open Access dell'Università di Torino

**Efficacy of the environmentally sustainable microwave heating compared to biocide applications in the devitalization of phototrophic communities colonizing rock engravings of Valle Camonica, UNESCO world heritage site, Italy**

**This is the author's manuscript**

*Original Citation:*

*Availability:*

This version is available <http://hdl.handle.net/2318/1809327> since 2023-03-17T16:21:12Z

*Published version:*

DOI:10.1016/j.ibiod.2021.105327

*Terms of use:*

Open Access

Anyone can freely access the full text of works made available as "Open Access". Works made available under a Creative Commons license can be used according to the terms and conditions of said license. Use of all other works requires consent of the right holder (author or publisher) if not exempted from copyright protection by the applicable law.

(Article begins on next page)

1 **Efficacy of the environmentally sustainable microwave heating compared to biocide**  
2 **applications in the devitalization of phototrophic communities colonizing rock engravings of**  
3 **Valle Camonica, UNESCO world heritage site, Italy**

4 Favero-Longo S.E.<sup>1,\*</sup>, Matteucci E.<sup>1</sup>, Pinna D.<sup>2,3</sup>, Ruggiero M.G.<sup>4</sup>, Riminesi C.<sup>3</sup>

5 <sup>1</sup> Università degli Studi di Torino, Dipartimento di Scienze della Vita e Biologia dei Sistemi,  
6 Viale Mattioli 25, 10125 Torino, Italy

7 <sup>2</sup> Università di Bologna, Dipartimento di Chimica ‘Giacomo Ciamician’, Via Selmi, 2, 40126  
8 Bologna BO

9 <sup>3</sup> CNR - Istituto di Scienze del Patrimonio Culturale (già Istituto per la Conservazione e  
10 Valorizzazione dei Beni Culturali), Via Madonna del Piano, 10 - 50019 Sesto Fiorentino (FI)

11 <sup>4</sup> Direzione Regionale Musei della Lombardia, Palazzo Litta, Corso Magenta, 24 - 20123 Milano

12

13 \*, corresponding author:

14 Sergio E. Favero Longo, PhD  
15 Università degli Studi di Torino  
16 Dipartimento di Scienze della Vita e Biologia dei Sistemi  
17 Viale Mattioli 25, 10125 Torino, Italy  
18 Tel. +390116705972  
19 Fax +390116705962  
20 sergio.favero@unito.it  
21 orcid.org/0000-0001-7129-5975

22

23

24 **Abstract**

25 The devitalization of lithobionts prior to their removal from engraved rocks is a common  
26 conservation practice periodically undertaken in rock art sites. In this study, we assessed *in situ* the  
27 efficacy of three traditional biocides and of an innovative microwave heating system, and compared  
28 different application protocols to devitalize foliose and crustose lichens and a cyanobacteria-  
29 dominated biofilm on the rock engravings of Valle Camonica (UNESCO site n.94, Italy). The  
30 analysis of their vitality and stress responses by monitoring chlorophyll *a* fluorescence parameters  
31 ( $F_v/F_m$ ,  $F_0$ , OJIP transient) showed that the common application of biocides by brush is rather  
32 ineffective, particularly in the case of the resistant crustose lichens. The heating of rock surfaces to  
33 70°C for a few minutes by the microwave system caused devitalization of lithobionts to a similar  
34 extent as the biocide application with cellulose poultice, which, however, introduced high amounts  
35 of chemicals in the environment. The microwave irradiation overcame any lithobiontic stress  
36 resistance and avoided useless or excessive spread of biocides, appearing a promising sustainable  
37 approach for the parallel conservation of rock art and its surrounding natural environment.

38

39 **Keywords:**

40 chlorophyll *a* fluorescence, environmentally safe art restoration, cyanobacteria, lichens, microwave,  
41 biocide

42

## 43 1. Introduction

44 Open-air rock art sites are exposed to human actions and natural processes which can affect their  
45 preservation, i.e. perpetuation of heritage asset, and conservation, i.e. physical lifetime (Darvill and  
46 Batarda Fernandes 2014). Natural threats of stone cultural heritage include lithobiotic (i.e. rock  
47 dwelling) microorganisms, which generally affect the aesthetic appearance and historic value and  
48 put at risk the conservation of artworks because of their biodeterioration potential (Pinna 2017;  
49 Favero-Longo and Viles 2020). In the case of engraved rocks, the spatial extension of physical and  
50 chemical interactions of lithobionts with the mineral substrate may be dimensionally similar to that  
51 of the heritage objects (e.g. rock paint or engraving) and should thus deserve special attention in  
52 management plans (Knight et al. 2004). The main public concern often relates to the aesthetic  
53 alteration caused by the lithobiotic covering which masks the appearance and alters the legibility  
54 of rock art surfaces to scholars and other visitors, thus affecting research activities and the tourism  
55 industry. Therefore, the removal of lithobiotic communities is a common periodic practice  
56 undertaken in many rock art sites. The simple mechanical removal of lithobionts from heritage  
57 surfaces mostly favors the persistence of live structures within the substrate and the spread of viable  
58 fragments thereof (Pinna 2017). Its effect in cleaning of rock art is generally only temporary  
59 (Tratebas 2004 with refs. therein). Treatments using biocides have thus been widely combined with  
60 mechanical cleaning, but only in a few cases the efficacy of the adopted protocols has been  
61 evaluated by experimental assays on the devitalization effects and supported by medium- and long-  
62 term monitoring programs of their impact on the surface stability and bioreceptivity (Tratebas 2004;  
63 Sanmartín et al. 2019). As the efficacy of biocide treatments against lithobionts is both species- and  
64 site-specific, biocides' assays need to be performed *in situ* and focused on the conservation threats  
65 of each site (Favero-Longo et al. 2017).

66 On the other hand, alternative and sustainable devitalization approaches are increasingly invoked to  
67 drastically reduce the use of chemicals, their potential interference with the rock substrates and their  
68 threats to humans and the whole biosphere (UNESCO 2008; Cappitelli et al. 2020; Sanmartín et al.  
69 2020). Recently, physical approaches have been experimented on rock art and other heritage  
70 surfaces by applying methods such as temperature shifts, electromagnetic radiations (e.g. gamma  
71 rays, UV, microwaves), and laser (Sanz et al. 2015; Pinna 2017 with refs. therein; Pozo-Antonio  
72 and Sanmartín 2018; Pozo-Antonio et al. 2019). Regarding temperature shifts, the heating of rock  
73 surfaces to 55-60°C, easily reached under direct sun radiation, is sufficient to devitalize lichens and  
74 other biodeteriogens within few hours if they are artificially kept fully hydrated (Tretiach et al.  
75 2012; Bertuzzi et al. 2013). However, the success of this approach strongly depends on the available  
76 sun radiation and, thus, on meteorological conditions, in a way that is hardly compatible with the  
77 planning of restoration interventions in temperate countries. The same approach was recently  
78 implemented shifting the energy input from the sun radiation to a microwave heating system (MW)  
79 suitable for usage in the field (Riminesi and Olmi 2016).

80 Microwave heating has already been applied to kill various targets, including insects and  
81 microorganisms threatening stored food materials and, more recently, heritage artefacts (Macana  
82 and Baik 2018; Cappitelli et al. 2020; Soni et al. 2020). Regarding the stone, a preliminary *in vitro*  
83 investigation highlighted the devitalization effect of MW on black fungi (Cuzman et al. 2013). Its  
84 potential has been also confirmed in the field on the easy geometries of tombstones (Mascalchi et  
85 al. 2015, 2020). However, the efficacy of microwaves against components of phototrophic  
86 communities colonizing rock art (lichens and cyanobacteria) needs to be proven. Moreover,

87 information is lacking on the application of MW on the irregular shapes of natural outcrops hosting  
88 rock art.

89 This work aimed to assess *in situ* the efficacy of different approaches, including traditional  
90 chemicals and the innovative MW, to devitalize lithobionts prior to their removal from engraved  
91 sandstone outcrops in the Rock Engravings National Park of Naquane in Valle Camonica, part of  
92 the UNESCO world heritage site n. 94 (Italy). Comparative assays encompassed (i) three  
93 commercial biocides and MW, (ii) different application methods, and (iii) three biological targets  
94 widespread in the site, namely a cyanobacteria-dominated phototrophic biofilm, crustose and  
95 foliose lichens. We tested the hypothesis that the same effects of traditional biocides may be  
96 obtained with the environmentally safe MW. The devitalization and the physiological resistance of  
97 lithobionts were evaluated measuring chlorophyll *a* fluorescence, an indicator of photosynthetic  
98 activity.

99

## 100 2. Materials & Methods

### 101 2.1. Study site and target species

102 Microwave and chemical treatments were performed on Rocks 30 and 31, respectively, of the Rock  
103 Engravings National Park of Naquane, in middle Valle Camonica [Capo di Ponte, Brescia, Italy:  
104 UTM ED50, N 5097692, E 604391; 475 m]. This intra-alpine area displays rainfall around 1000  
105 mm yr<sup>-1</sup> and air temperatures ranging from av. 2°C in winter to av. 21°C in summer (monitoring  
106 station n. 129 of ARPA Lombardia, Capo di Ponte, 342 m a.s.l., dataset 2003-2016). Petroglyphs  
107 are carved in sandstone outcrops of the Verrucano Lombardo Formation (Upper Permian; Brack et  
108 al. 2008), which are widely colonized by phototrophic biofilms and lichens. Coccoid (*Gloeocapsa*  
109 sp., *Chroococcus* sp.) and filamentous (*Scytonema* sp., *Stigonema* sp.) cyanobacteria are the main  
110 components of biofilms, also including green algae, primordia of lichen thalli and microcolonial  
111 black fungi. Foliose thalli of *Xanthoparmelia* [mostly *X. conspersa* (Ach.) Hale] and mesophytic  
112 crustose species [mostly *Circinaria caesiocinerea* (Malbr.) A. Nordin, Savić & Tibell, *Pertusaria*  
113 *flavicans* Lamy, *Rhizocarpon disporum* (Hepp) Müll. Arg., and *Rufoplaca* gr. *arenaria* (Pers.)  
114 Arup, Söchting & Frödén,] are the dominant species in the lichen communities (Favero-Longo and  
115 Matteucci 2022).

116 Documentation available on cleaning interventions in the Park (irweb.it), registered from early  
117 1980s, does not mention Rocks 30 and 31. Thus they have been likely left uncleaned for not less  
118 than 40 years. Treatments were performed on 15-30 cm × 15-30 cm parcels on the phototrophic  
119 biofilm, and on selected mature thalli of the foliose lichen *Xanthoparmelia conspersa* and the  
120 crustose *Rufoplaca* gr. *arenaria* (Fig. S1a).

121

### 122 2.2. Biocide application

123 The three biocides were prepared following the manufacturer's instructions as follows: 2%  
124 Preventol RI80 ® (benzalkonium chloride, ~80%, as active principle; Lanxess, Köln, Germany) in  
125 water, 3% Biotin T ® (N-octyl-isothiazolinone, 7-10%, and didecyl-dimethyl ammonium chloride,  
126 40-60%, as active principles; CTS, Altavilla Vicentina, Italy) in deionized water, and 3% Biotin R  
127 ® (N-octyl-isothiazolinone, 3-5%, and 3-iodo-2-propynyl butylcarbamate, 10-25%, as active  
128 principles; CTS) in white spirit. Professional restorers applied the biocides in April 2018 on the  
129 phototrophic biofilm and lichens pre-hydrated with sprayed water (Favero-Longo et al. 2020). The

130 application was carried out using a paintbrush (Fig. S1b) and a cellulose poultice (Fig. S1c). The  
131 poultice was removed using a small spatula after 4 h, and then the treated thalli and biofilms were  
132 gently washed with tap water. Deionized water only was also separately applied as negative control.  
133 Three replicates per target organism (*X. conspersa*, *R. arenaria*, phototrophic biofilm) per product  
134 (deionized water, DW; Preventol, PV; Biotin T, BT; Biotin R) per application method (brush,  
135 poultice) were examined [equivalent to a total of 72 assays].

136

### 137 2.3. Microwave application

138 A portable microwave system for localized surface and sub-surface treatment (Fig. 1a) was  
139 employed in this study (Riminesi and Olmi 2016). Its antenna, subsequently designated as  
140 ‘applicator’, consists of a truncated rectangular waveguide with a properly designed slot on the  
141 aperture. The geometry of the applicator allows the devitalization of lithobiontic microorganisms,  
142 growing on and beneath stone surfaces, by concentrating the microwave field distribution on a  
143 semi-ellipsoidal volume of the treated material, with an elliptical surface footprint  $4\text{cm} \times 3\text{cm}$  in  
144 size and a depth of approx. 1.5 cm (Riminesi and Olmi 2016). A key aspect of the method is that  
145 microwave radiation heats targets containing water, allowing the selective treatment of living cells  
146 with a higher water content than that of the materials hosting the organisms..

147 The treatment was performed in June 2019 with two application methods: the applicator placed in  
148 direct contact with the colonized rock (Fig. 1b) and on a layer of cellulose poultice moistened with  
149 water (Fig. S1c). In both cases, the rock surface and the lithobionts were previously moistened with  
150 sprayed water. Heating of the rock surface was monitored in real-time by a non-conductive fiber  
151 optical sensor (Luxtron 1000A/A with fluoroptic probe; Luxtron, Cuneo, Italy). The microwave  
152 application was stopped when the rock surface had reached the threshold of  $70^\circ\text{C}$  for  $170 \pm 4$  sec,  
153 which was recognized as the best microwave dose against other lithobionts (that is black fungi;  
154 Cuzman et al. 2013). The cellulose poultice was removed a few minutes after the microwave  
155 application and the surface was gently washed with tap water.

156 Three replicates per target organism per application method were examined [ $n = 18$ , equivalent to 3  
157 target organisms  $\times$  2 application methods  $\times$  3 replicas].

158

### 159 2.4. Vitality measurements

160 Chlorophyll *a* fluorescence ( $\text{Chl}_a\text{F}$ ) of phototrophic biofilms and lichens was quantified 4-6 hours  
161 before ( $T_0$ ), 24 hours ( $T_1$ ) and 40 ( $T_{40}$ ) days after the treatments. In particular, the monitoring of  
162 biocide effectiveness was performed on April 10<sup>th</sup> ( $T_{0B}$ , where “B” stands for “Biocides”), April 11<sup>th</sup>  
163 ( $T_{1B}$ ) and May 19<sup>th</sup> ( $T_{40B}$ ) 2018, and that of microwave effectiveness on June 20<sup>th</sup> 2019 ( $T_{0M}$ ,  
164 where “M” stands for “Microwaves”), June 21<sup>st</sup> ( $T_{1M}$ ) and July 30 ( $T_{40M}$ ) 2019. Although the  
165 monitoring of biocide and microwave assays was not performed at the same time due to logistic  
166 constrains, the rather similar mild and rainy climate conditions of the study area in central-spring  
167 ( $T_{0B}$ - $T_{40B}$ ) and early-summer ( $T_{0M}$ - $T_{40M}$ ) periods (Fig. S2) were considered acceptable to analyze  
168 the treatment effects on similarly active lithobiontic targets. Nevertheless, any differences in the  
169 starting photosynthetic efficiency observed at  $T_{0B}$  and  $T_{0M}$  were taken into account in the  
170 evaluation of biofilm and lichen responses (sections 3.1 and 4.1).

171  $\text{Chl}_a\text{F}$  was measured with a Handy-PEA fluorimeter (Hansatech Instruments Ltd., Norfolk,  
172 England; saturating light pulse of 1s,  $1500 \mu\text{mol m}^{-2}\text{s}^{-1}$ , peak at 650 nm) on moistened thalli and  
173 biofilms, previously obscured with a black fabric for twenty minutes to allow dark-adaptation. All

174 measurements were collected early in the morning, before the stone heating by sun, except for those  
175 at T40<sub>B</sub>, which were performed late in the morning, when air temperature was approx. 20°C, but the  
176 sun radiation had already started to warm the rock surface. At each time point, five measurements  
177 were performed on each thallus of *X. conspersa* and *R. arenaria*, and on the biofilm parcels. The  
178 maximum quantum yield of PSII ( $F_v/F_m$ , with  $F_v=F_m-F_0$ ,  $F_0$  and  $F_m$  = the minimum and maximum  
179 fluorescence, with all reaction centres open and closed, respectively), indicates the functionality of  
180 the photosynthetic process and, thus, the general level of phototrophic lithobionts' fitness (Tretiach  
181 et al. 2010, 2012).  $F_0$ , which is related to the chlorophyll *a* content (Sanmartín et al. 2019), was also  
182 monitored. The threshold 0.15 of  $F_v/F_m$  values and the decrease of  $F_0 >80\%$  were considered as  
183 reference values for devitalized lichens, that is, when their metabolic recovery can be confidently  
184 ruled out (Favero-Longo et al. 2017 with refs. therein). Moreover, the OJIP transient was examined,  
185 that is the Chl<sub>a</sub>F polyphasic curve from  $F_0$  (O) to  $F_m$  (P), with two steps at 2 ms (J) and 30 ms (I).  
186 The very fast O to J phase (photochemical phase) is mostly due to the reduction of the primary  
187 acceptor quinone of PSII ( $Q_A$ ), being indicative of antenna size and connectivity of PSII reaction  
188 centres (Stirbet and Govindjee 2011; Malaspina et al. 2015). The J to I and I to P rises (thermal  
189 phase) are associated to the reduction of the plastoquinone-pool centers and the electron flow  
190 through PSI, respectively (Stirbet and Govindjee 2011; Malaspina et al. 2015). Another inflection is  
191 sometimes observed at 300  $\mu$ s (K-step) as a response to thermal stress, attributed to the inactivation  
192 of the oxygen-evolving complex (Strasser 1997; Stirbet et al. 2019). The study of the O(K)JIP curve  
193 thus contributes to understand the impact of stress factors on the structure and functioning of the  
194 photosynthetic apparatus.

195 As a complement of Handy-PEA measurements, the responses of lichens and the phototrophic  
196 biofilms observable with the naked eye were visually monitored and recorded using the digital  
197 camera of an iPhone 5. Moreover, lobes of *X. conspersa* thalli were cut with a lancet at T0, T1 and  
198 T40, cross-sectioned and observed using an epifluorescence microscope Nikon Eclipse 300 to  
199 obtain spatial information on the devitalization of the photobiont layer (Favero-Longo et al. 2017).

200

## 201 2.5. Statistics

202 A factorial ANOVA was used to detect significant differences in Chl<sub>a</sub>F parameters ( $F_v/F_m$ ,  $F_0$ )  
203 according to the following independent variables: type of treatment (DW, PV, BT, BR, MW), time  
204 point (T0, T1, T40), application method (brush/direct, cellulose poultice), and target lithobiont (*X.*  
205 *conspersa*, *R. arenaria*, phototrophic biofilm). For each treatment, significant differences in  $F_v/F_m$   
206 and  $F_0$  values at the different time points were analyzed by ANOVA with post-hoc Tukey's test  
207 ( $P<0.05$  as significant). As for microwave treatments, the times needed to reach temperature  
208 thresholds fixed from 30°C to 80°C (at each 5°C interval) when the applicator was applied directly  
209 on the rock surface or with the cellulose poultice were compared by ANOVA with post-hoc t-test,  
210 and time intervals of the exposition to temperatures higher than thresholds fixed from 30°C to 80°C  
211 (at each 10°C interval) were compared for the different study cases (target organisms  $\times$  application  
212 methods) by ANOVA with post-hoc Tukey's test. All these analyses were carried out using  
213 SYSTAT 10.2 (Systat Software Inc., San Jose, CA).

214 The shapes of OJIP curves were compared using the PEA Plus 1.12 software package (Hansatech  
215 Instruments Ltd., UK).

216

217

## 218 3. Results

### 219 3.1. *Chl<sub>a</sub>f* of lichen thalli and the biofilm before treatments

220 *Chl<sub>a</sub>f* of the lichen thalli and of the biofilm was measured before the treatments with biocides and  
221 microwaves in April (T<sub>0B</sub>) and June (T<sub>0M</sub>), respectively. Negative controls (deionized water  
222 treatments) were monitored between April (T<sub>0B</sub>) and May (T<sub>40B</sub>) in parallel with biocide  
223 treatments.

224 The  $F_v/F_m$  values (Fig. 2) of negative controls were uniform at the different time points (T<sub>0B</sub>, T<sub>1B</sub>,  
225 T<sub>40B</sub>), but differed significantly between biological systems (*X. conspersa*, av. 0.68 > *R. arenaria*,  
226 av. 0.44 > cyanobacterial biofilm, av. 0.26). Similarly,  $F_0$  was higher in the foliose lichen thalli (av.  
227 85) than in the crustose ones (av. 35) and the phototrophic biofilm (av. 22) (Fig. 3).  $F_0$  values of the  
228 lichens and the biofilm measured at T<sub>0M</sub> were generally higher than those measured at T<sub>0B</sub>.

229 The fluorescence transient curves of untreated *X. conspersa* (negative controls, and T<sub>0B</sub> and T<sub>0M</sub> of  
230 the different assays; Fig. 4a and Fig. S3a) showed the typical OJIP shape, as expected for unstressed  
231 thalli. A remarkable increase of  $F_0$  and  $F_M$ , and of the whole amplitude of the curve, was observed  
232 at T<sub>0M</sub> with respect to T<sub>0B</sub>. *R. arenaria* (Fig. 4b and Fig. S4a) similarly showed the characteristic  
233 sequence of the OJIP steps at T<sub>0M</sub>, while  $F_0$ ,  $F_M$  and the amplitude of the curve were remarkably  
234 lower at T<sub>0B</sub>. At this time, a first peak along the curve was observed at 300  $\mu$ sec (K-step), less  
235 pronounced or absent at T<sub>0M</sub>. At T<sub>40B</sub>, the negative controls of both lichens showed an anticipation  
236 of the P phase, observed at 0.3 sec. rather than at 0.5 sec.

237 The fluorescent transient curves of the biofilm were of much lower amplitude than those of the  
238 foliose and crustose lichens (Fig. 4c and Fig. S5a).  $F_0$  and  $F_M$  were higher at T<sub>0M</sub> than at T<sub>0B</sub>. At  
239 this latter time, in particular, the amplitude of the IP phase was minimal, while it was better  
240 recognizable, in the series of negative controls, at T<sub>40B</sub>. A K-step was observed at both T<sub>0B</sub> and  
241 T<sub>0M</sub>.

242

### 243 3.2. Heating of the rock surfaces treated with microwave radiation

244 Real-time temperature monitoring of the surfaces treated with microwaves is summarized in Fig. 5.  
245 All the parcels were exposed to rather similar heating rates, with the rock surface temperature  
246 quickly increasing to 50°C (after 19±6 sec, mean±SD), 60°C (45±10 sec), and 70°C (104±21 sec)  
247 (Fig. 5a). All the parcels were exposed to a temperature higher than 50°C for approx. 240 sec and to  
248 a temperature equal or higher than 70°C for approx. 170 sec (Fig. 5b). The heating rate was slightly  
249 faster for the parcels covered with cellulose poultice (Fig. 5a). Therefore, the total irradiation time  
250 on these parcels was shorter than that of the parcels treated with the applicator in direct contact  
251 (particularly in the case of *R. arenaria*), and temperatures even briefly increased above 80°C.

252

### 253 3.3. Effects of biocides and microwave heating on *Chl<sub>a</sub>f*

254 At T<sub>40</sub>, each lithobiont treated with chemicals or MW exhibited a modified appearance in  
255 comparison to T<sub>0</sub> and the controls, observable with the naked eye. The thalli of *X. conspersa* were  
256 yellowed (Fig. 1d-e and Fig. S6), those of *R. arenaria* appeared crumpled (Fig. S7), and the  
257 phototrophic biofilm exhibited wide detachments (Fig. S8). These modifications occurred



258 regardless the treatment type and the application method. However, such homogeneity in the visible  
259 effects was not reflected by Chl<sub>a</sub>F responses.

260 The factorial ANOVA showed that all the examined variables (type of treatment, time, target  
261 lithobiont, application method) significantly contributed to the devitalization effectiveness, as  
262 expressed by the  $F_v/F_m$  and  $F_0$  parameters (Table S1). Both chemicals and MW devitalized the  
263 target lithobionts, but the efficacy strongly depended on the application method.

264 After the application of the biocides by brush,  $F_v/F_m$  values of *X. conspersa* and *R. arenaria*  
265 remarkably decreased at T1<sub>B</sub> (-65% to -95%, out of Preventol on *X. conspersa*), but at T40<sub>B</sub> they  
266 showed a significant recovery above the vitality threshold of 0.15 (Fig. 2).

267 Uniquely, brush application of Preventol (PV) and Biotin T (BT) zeroed the median  $F_v/F_m$  values of  
268 the phototrophic biofilm, which was instead generally unaffected by Biotin R (BR).  $F_0$  values of  
269 *Xanthoparmelia* at T40<sub>B</sub> were much lower than those at T0<sub>B</sub> and T1<sub>B</sub>, but they neither zeroed nor  
270 decreased more than 80% (Fig. 3). Such fluorimetric results were also confirmed by epifluorescence  
271 microscopy, displaying the persistence of residual, red autofluorescent viable cells in the lower part  
272 of the photobiont layer (Fig. S9). *R. arenaria* and the biofilm treated with PV and BT showed a  
273 considerable increase of  $F_0$  values at T1<sub>B</sub> and a decrease at T40<sub>B</sub>. Only the biofilm showed zeroed  
274  $F_0$  values after PV application.

275 On the contrary, both lichens and the biofilm were strongly affected by all the chemicals when  
276 applied by the cellulose poultice. In all cases (out of PV on *R. arenaria*),  $F_v/F_m$  values at T40<sub>B</sub>  
277 were much lower than 0.15, and in most cases the strong devitalization effect was already detected  
278 at T1<sub>B</sub>.  $F_0$  values of *X. conspersa* at T40<sub>B</sub> strongly decreased (>80%) being quite zeroed. Regarding  
279 *R. arenaria* and the biofilm, the relative increase of  $F_0$  at T1<sub>B</sub> was mostly followed at T40<sub>B</sub> by a  
280 strong decrease (>80%) and/or by zeroing of median values (with the confirmed exception of PV on  
281 *R. arenaria*).

282 The microwave heating system also showed different efficacies when applied directly on the rock or  
283 with the interposed layer of cellulose poultice. The direct application was very efficient, with  $F_v/F_m$   
284 values of all lithobionts decreasing below 0.15 since T1<sub>M</sub> and zeroing at T40<sub>M</sub> in the case of *X.*  
285 *conspersa* and the biofilm. The zeroing of  $F_0$  values at T40<sub>M</sub> confirmed the result. By contrast, MW  
286 application on the surfaces covered by the cellulose poultice was only effective on *X. conspersa*  
287 ( $F_v/F_m < 0.15$  at T1<sub>M</sub> and T40<sub>M</sub>;  $\Delta F_0 > 80\%$ ). Both *R. arenaria* and the biofilm showed a low increase  
288 of  $F_0$  at T1<sub>M</sub> and only a limited decrease of  $F_v/F_m$  and  $F_0$  values at T40<sub>M</sub>.

289 Fluorescent transient curves confirmed the importance of the application method on the efficacy of  
290 biocides (Figs. S3-S5) and microwave radiation (Fig. 4). The poultice application of biocides (Fig.  
291 S3) and the direct application of MW on *X. conspersa* (Fig. 4a) led to the flattening of the curve  
292 since T1<sub>B,M</sub> and to its zeroing at T40<sub>B,M</sub>. The application by brush of BR similarly flattened the  
293 curve at T1<sub>B</sub>, while a minimal amplitude, with the appearance of a K-step at 300  $\mu$ sec, was still  
294 observed with BT; a slight rise of the OJ phase and a reduction of the IP amplitude were observed  
295 with PV (Fig.S3). For all the biocides, a minimum curve amplitude was still observed at T40<sub>B</sub>, with  
296 the OJ and IP phases recognizable for BT  $\gg$  BR  $>$  PV (Fig. S3). MW application with the  
297 interposed layer of cellulose poultice determined the increase of  $F_0$ , but flattened the curve, which  
298 definitely zeroed at T40<sub>M</sub> (Fig. 4a).

299 BR and BT poultices (Fig. S4) and MW direct application (Fig. 4b) on *R. arenaria* determined at  
300  $T_{0_{B,M}}$  an increase of  $F_0$  and the flattening of the curve, which was still flattened and zeroed at  
301  $T_{40_{B,M}}$ . PV poultice also flattened the curve at  $T_{1_B}$ , without the increase of  $F_0$ , but it recovered  
302 some amplitude and the characteristic OJIP steps at  $T_{40_B}$ , with a well-defined K-step at 300  $\mu\text{sec}$   
303 (Fig. S4). Biocides applied by brush (Fig. S4) and the MW indirect application (Fig. 4b) also  
304 resulted in a strong reduction of the curve amplitude, with a remarked K-step and the flattening of  
305 the IP phase (and for BT and PV the increase of  $F_0$ ). However, all the thalli recovered the  
306 characteristic OJIP steps at  $T_{40_{B,M}}$ , more remarkably for BT,  $MW > BR, PV$ .

307 Regarding the phototrophic biofilm, all the biocides caused an increase of  $F_0$  and  $F_M$  at  $T_{1_B}$ .  
308 Poultice applications were characterized by a complete curve flattening, while a minimal  
309 preservation of the OJ rise and of the K-step followed the brush treatment (Fig. S5). At  $T_{40_B}$ , the  
310 fluorescent transient was flat and zeroed for PV treatments, flat for BT treatments (but with  $F_0$   
311 around 10), and flat and zeroed for the poultice application of BR, while the OJ rise was still  
312 observed with brush. With the MW direct application (Fig. 4c),  $F_0$  and  $F_M$  decreased since  $T_{1_M}$ , and  
313 the fluorescent transient was flattened and zeroed at  $T_{40_M}$ . The MW indirect treatment increased  $F_0$   
314 and  $F_M$  values at  $T_{1_M}$ , with some curve amplitude remaining, that is a profile similar to those  
315 observed with biocide treatments. The OJ rise was still observable also at  $T_{40_M}$ .  
316 It is worth noting that both chemical and MW applications, independently of their devitalization  
317 efficacy, did not directly lead to the complete removal of targeted lithobionts, which instead  
318 required successive interventions with mechanical tools to gently detach both lichen thalli and the  
319 phototrophic biofilm, and thus achieve surface cleaning (Fig. 1f).  
320

#### 321 4. Discussion

322 The devitalization of lithobionts before their removal has long been recognized as a necessary step  
323 to assure the efficacy and durability of cleaning procedures on engraved rock surfaces (Tratebas  
324 2004). Unfortunately, if a biocide treatment fails to devitalize the target lithobionts, the restoration  
325 would be ineffective and unjustifiably pollutive too, because of the useless spread of chemicals in  
326 the environment. This drawback may be particularly critical when using biocides containing  
327 benzalkonium chloride, which was suggested to serve as a nutrient to microorganisms due to its  
328 nitrogen content, thus favoring recolonization dynamics (Scheerer et al. 2009), and to promote the  
329 selection of resistant microbial strains (Martin-Sanchez et al. 2012; Kim et al. 2018).

330 This work showed that the application of biocides on rock art surfaces by brush -a commonly  
331 practiced devitalization procedure saving time and materials- can be ineffective on resistant  
332 lithobionts, as crustose lichens are (Table 1). Moreover, our results confirmed the hypothesis that  
333 the heating of rock surfaces to 70°C for a few minutes by a microwave system causes the same  
334 effective devitalization of the targeted lithobionts obtained with the cellulose poultice application of  
335 biocides. It is worth mentioning that this latter approach introduces in the substrate higher amounts  
336 of biocides than the brush application (Favero-Longo et al. 2020), with consequent environmental  
337 concern. Heating by microwave radiation does not leave any residual on the substrate. When  
338 exposed to the oscillating microwave field, the water molecules of both lithobionts and the stone  
339 move (ionic conduction) and rotate (dipolar rotation), with their frictions resulting in heat  
340 generation and increase of temperature. After removing the microwave applicator, the molecules  
341 stop moving and vibrating, and the temperature comes back rapidly, without leaving any residual

342 effect, by emitting blackbody radiation in IR range (9-12  $\mu\text{m}$ ) or dissipating their heat by  
343 conduction (Metaxas and Meredith 2011). Accordingly, microwave irradiation does not impact rock  
344 surfaces with temperature shifts similar to those used in pulsed laser irradiation, which instead may  
345 cause thermal stress and the melting of rock-forming minerals (De Cruz et al. 2014; Pozo-Antonio  
346 et al. 2019).

347 At present, the portable microwave system (MW) only allows the irradiation of small surfaces, as it  
348 is necessary to perform multiple adjacent applications of the 4 cm  $\times$  3 cm applicator, each taking  
349 approx. 5 minutes to reach and maintain 70°C for approx. 3.0 minutes. This means that the device  
350 takes approx. 6-7 hours to cover 1 m<sup>2</sup>, a treatment rate unsuitable to cover the wide outcrops of rock  
351 art sites, but effective to treat lithobionts on small, engraved rock areas of peculiar interest. The  
352 MW instrumentation is being developed further to allow treatments of larger surfaces. Here we  
353 discuss the species-specific efficacy of physical and chemical devitalization treatments in relation to  
354 the different physiological responses of target lithobionts, addressing critical issues for the  
355 management of rock art and the surrounding natural environment. A first insight on the microwave  
356 effects on the photosynthetic efficiency of lichens and cyanobacteria is provided.

357

#### 358 4.1. Photosynthetic efficiency of target lithobionts

359 Different values of  $F_0$  (and  $F_v/F_m$ ) for each species at  $T_{0B}$  and  $T_{0M}$  indicated a seasonality of the  
360 photosynthetic performance, which has been previously reported for saxicolous lichens of the  
361 Mediterranean region, showing a marked reduction of quantum efficiency in summer drought  
362 periods, followed by the recovery of their optimum fluorescence in autumn (Vivas et al. 2017).  
363 However, the present study showed that lower  $F_0$  and  $F_v/F_m$  values at  $T_{0B}$  than at  $T_{0M}$  were  
364 measured in a humid week of a wet spring (as usual in Valle Camonica; see Gerosa et al. 2013;  
365 cumulative rain in Oct17-Jul18 in Fig. S2b). Higher  $F_0$  values and higher amplitude of OJIP curves  
366 registered at  $T_{0M}$  (cumulative rain in Oct18-Jul19 in Fig. S2b) may be thus better explained by a  
367 recovery of the photobiont populations in the vegetative season, which determined a higher  
368 chlorophyll content in the thalli (Baruffo and Tretiach 2007), rather than by the absence of drought  
369 stress.

370 Different  $F_0$  and  $F_v/F_m$  values at  $T_{0B,M}$  of *X. conspersa* and *R. arenaria* indicated the well-known  
371 interspecific variability of the lichen photosynthetic performances, with lower values reported more  
372 often in crustose than foliose species (Jensen et al. 2002). However, although foliose species may be  
373 expected to harbour more photobionts and thus contain higher chlorophyll contents than crustose  
374 ones, the photosynthetic performance seems to be not uniquely related to growth form, but also  
375 influenced by the substratum and the microenvironmental conditions (Nayaka et al. 2009).  
376 Accordingly, the direct contact of *R. arenaria* with the rock may regularly determine stressful  
377 conditions, revealed by the small K-step observed along the OJIP curve already at  $T_{0B,M}$ , and  
378 instead not detected in *X. conspersa*, in which the rhizinae are interposed between the rock and the  
379 thallus. In plants, the K-step has been related with a heating induced injury in the oxygen-evolving  
380 complex of PSII, determining an imbalance in the electron flow around P680 and the accumulation  
381 of oxidized reaction centers (Strasser 1997; Kalaji et al. 2016). Small K-steps as observed in this  
382 study for *R. arenaria*, even before any treatment, usually characterize highly stressed organisms  
383 (Marečková et al. 2019). Surprisingly, the K-step was not observed in *X. conspersa* even at  $T_{40B}$ ,

384 when the measures were performed late in the morning of a sunny day, and the fluorescent transient  
385 was thus affected in the IP phase.

386  $F_v/F_m$  values of the phototrophic biofilm at  $T_{0B,M}$  (av. 0.26) were only slightly lower than maximum  
387 values reported for cyanobacteria *in vitro* (0.3-0.4; Gao et al. 2007). Such low values were obtained  
388 using the “apparent”  $F_0$  and  $F_M$  values, that were measured not considering that cyanobacteria,  
389 unlike green algae and higher plants, use electron flows from PSII in both photosynthesis and  
390 respiration (Stirbet et al. 2019). Approaches to obtain more reliable  $F_v/F_m$  values (reviewed in  
391 Stirbet et al. 2019) were not followed here, as the devitalization was evaluated by adopting the same  
392 measuring conditions before and after both treatments. Similarly to lichens, the K-step at 300  $\mu$ sec  
393 is a marker of heat stress in cyanobacteria (Zhang and Liu 2016; Kvíderová and Kumar 2020). It  
394 was observed in the measures of the phototrophic biofilm even before the devitalization treatments.  
395 Accordingly, the phototrophic biofilm and *R. arenaria*, more adherent to the rock, appeared  
396 regularly affected by heat stress, while *X. conspersa* was not.

397

#### 398 4.2. Microwave heating and photosynthetic efficiency

399 The application of microwave heating directly on the rock surface moistened with sprayed water  
400 overcame the stress tolerance of all the lithobionts, with flattened fluorescent curves at  $T_{1M}$ , which  
401 did not show any recovery at  $T_{40M}$  likely because of the high temperature of the irradiated surface.  
402 Indeed, 70°C could be tolerated by lichens when dry (Lange 1953), but not in the hydrated state,  
403 when their heat resistance ranged from 35° to 46°C (MacFarlane and Kerhaw 1980; Tretiach et al.  
404 2012). The cyanobacteria-dominated phototrophic biofilm did not show the resistance demonstrated  
405 by certain epilithic green-algae, which survived even in the hydrated state to a heat-shock treatment  
406 at 60°C, as few unaffected cells re-established viable populations (Bertuzzi et al. 2017). MW  
407 application with the interposed poultice layer gave a better glimpse of the lithobiontic response to  
408 the heating stress. Together with the  $F_m$  decrease, the stress was indicated by  $F_0$  increase in *X.*  
409 *conspersa* > phototrophic biofilm > *R. arenaria*, which may depend on the heat-induced presence of  
410 free chlorophyll and uncoupled antennas proteins (Strasser 1997). Remarkably, the lower  $F_0$   
411 increase showed by the lithobionts more adherent to the substrate, and likely more used to heat  
412 stress than *X. conspersa* (MacFarlane and Kershaw 1980), corresponded to their higher recovery at  
413  $F_{40M}$ . Accordingly, in laboratory experiments simulating some microclimatic conditions of the  
414 warm Namib desert, the hydrated thallus of genus *Xanthoparmelia* (*X. walteri*) was still  
415 photosynthetically active at 55°C, while that of genus *Caloplaca* (*C. elegantissima*, sharing with *R.*  
416 *arenaria* the former genus *Caloplaca* s.l., before its recent subdivision based on molecular  
417 phylogeny; Arup et al. 2013), was inactive above 45°C; nevertheless, the latter species was the most  
418 widespread in the real desert, suggesting that its response implied some adaptation to this harsh  
419 environment (Lalley and Viles 2006; see next section). On the other hand, although the different  
420 lithobionts were exposed for the same time interval to 70°C and more, the different heating rate of  
421 each surface corresponded to a different total time of microwave irradiation. In particular, the  
422 duration was generally lower for the less effective poultice application, with the higher water  
423 availability likely accounting for the higher heating rates (Metaxas and Meredith 2011). The  
424 shortest irradiation interval and exposition to 40-60°C (but also the highest interval above 80°C)  
425 were observed for the poultice application on the more resistant *R. arenaria*. Accordingly, the time  
426 of exposition to temperatures around the limit of photosynthetic activity (approx. 50°C) may be

427 even more crucial in terms of treatment effectiveness than the high temperature (equal or above  
428 70°C) at which lithobionts are metabolically inactive and thus more tolerant to stress (Lalley and  
429 Viles 2006).

430

#### 431 4.3. Biocides and photosynthetic efficiency

432 The higher resistance of *R. arenaria* > phototrophic biofilm > *X. conspersa* was also confirmed by  
433 the results of biocide treatments, although there were some different patterns depending on the  
434 product.  $F_v/F_m < 0.15$  and the flattening and zeroing of the transient curve in *R. arenaria* were  
435 observed only after the application of BR and BT by poultice. These biocides contain  
436 isothiazolinones, which yield metabolic inhibition by targeting thiol-containing enzymes (Denyer  
437 and Stewart 1998). PV contains benzalkonium chloride (BZC), which damages biological  
438 membranes and causes cell lysis (Wessels and Ingmer 2013). Unlike the other two biocides, PV did  
439 not cause the devitalization of the crustose lichen. Although the transient curve was rather flat at  
440  $T_{1B}$ , it recovered the OJIP shape at  $T_{40B}$ , including a small K-step, suggesting that the resistance to  
441 heating stress is suitable to provide resistance also to the biocidal action of the quaternary  
442 ammonium salt. This does not mean that quaternary ammonium salts did not affect the photobionts,  
443 because after the application by brush of PV and BT, which contain BZC and didecyl-dimethyl  
444 ammonium chloride, respectively, an increase of  $F_0$  was observed at  $T_{1B}$ , possibly related to the  
445 occurrence of free chlorophyll caused by the membrane perturbation (Strasser 1997). However, this  
446 effect likely did not occur in the whole photobiont layer and was therefore ineffective. Similarly,  
447 another species of the genus *Caloplaca* s.l. (*Variospora aurantia*) was shown to preserve viable  
448 algae in some parts of the photobiont layer after the poultice application of BZC (1.5%) on  
449 carbonate blocks in a semi-arid environment, where lichens usually tolerate remarkable thermal and  
450 salt stresses (Matteucci et al. 2019). Differently, poultice applications of PV, and of the other two  
451 biocides, effectively devitalized the photobionts of *X. conspersa*, and also those of the crustose  
452 lichen *Verrucaria nigrescens* and of the placodioid *Protoparmeliopsis muralis*, which also  
453 frequently occur on heritage surfaces (Favero-Longo et al. 2017). The hypotheses that the  
454 *Trebouxia* photobionts involved in the symbiosis with the *Caloplaca* mycobionts are more stress  
455 resistant than those of *Xanthoparmelia* and others, or that the *Caloplaca* mycobionts confer more  
456 protection to their photobionts, allowing their resistance, appear worth to be investigated. Several  
457 species of genus *Caloplaca* s.l. display fungal and algal stacks as an adaptation to strong light  
458 radiation (Vondrák and Kubásek 2013), which may also confer tolerance to other stress factors.

459  $F_0$  increased at  $T_{1B}$  when PV and BT were applied by brush, but not when applied by poultice. The  
460 result suggests that its initial rapid increase, caused by membrane damages, was still detectable the  
461 day after the application of a low amount of biocide, while it was followed by a quick decrease due  
462 to the more abundant amount of biocide. By contrast,  $F_0$  increased only with the poultice  
463 application of BR, and it might be caused by the effect of white spirit solvent, as the same was  
464 observed when it was applied alone as control (not shown).

465 The biocide application by brush on both lichens was always followed by the recovery of  
466  $F_v/F_m > 0.15$  and of the OJIP shape of the transient curve, more remarkable for *R. arenaria*,  
467 indicating the poor suitability of this method on potentially resistant crustose species such as those  
468 of genus *Caloplaca* s.l. By contrast, some higher efficacy was observed when PV and BT were

469 applied by brush on the cyanobacteria-dominated biofilm. This result is of remarkable interest as  
470 these lithobiontic communities widely covered the surfaces, and it is therefore difficult (and not  
471 environmentally safe) to plan a poultice application at the scale of the whole outcrops. The result is  
472 partially explained by the different hydrophilicity displayed by biofilms depending on the  
473 composition of their extracellular polymeric substances (EPS; Sanmartín et al. 2020), which in the  
474 examined case likely did not prevent the absorption of the water-dissolved quaternary ammonium  
475 salts. The cyanobacterial cell membranes, not protected by the mycobiont as lichen green algae are,  
476 were eventually damaged. Accordingly, a strong  $F_0$  increase was observed at T1<sub>B</sub>, after both brush  
477 and poultice applications, suggesting again the presence of free chlorophyll (Strasser 1997). This  
478 finding agrees with the positive results of PV applied on cyanobacteria on carbonate rocks, causing  
479 the complete disorganization of the prokaryotic cells (Ascaso et al. 2002), and with the significant  
480 decrease of chlorophyll *a* observed in planktonic cyanobacterial cultures (*Nostoc* sp.) treated with  
481 BT (Sanmartín et al. 2015). Oppositely, in this study, the phototrophic biofilm showed a better  
482 resistance to BR application by brush than that of BT, contrasting with previous findings about its  
483 treatment on carbonate substrates (de los Ríos et al. 2012). This result may depend on the different  
484 substrates and/or a diverse composition and hydrophilicity of the EPS, which may together  
485 influence the biocide availability and absorption (Favero-Longo et al. 2020; Sanmartín et al. 2020).

486 It is finally worth noting that all these different patterns of resistance or sensitivity to the various  
487 treatments were detected and quantified with the fluorimetric measures, which are confirmed as a  
488 crucial tool to assess the efficacy of devitalization protocols against phototrophic lithobionts, and  
489 validate their adoption in restoration interventions (Tretiach et al. 2010). By contrast, the sole  
490 observation of treated lithobionts with the naked eye may reveal a similar appearance for  
491 devitalized and (partially) live thalli and biofilms and it is thus not a reliable feedback to select  
492 effective strategies for biodeterioration control.

493

## 494 **5. Conclusions**

495 This work demonstrated that microwave heating represents an effective and sustainable method to  
496 devitalize cyanobacterial biofilms, crustose and foliose lichens that grow on the rock engravings of  
497 Valle Camonica, yielding the same successful devitalization obtained by an abundant biocide  
498 application, but avoiding any dispersal of toxic residues in the environment.

499

## 500 **6. Acknowledgements**

501 This research has been carried out in the framework of the project “Monitoring of, and Good  
502 Practices for, the protection of UNESCO site 94 Rock art in Valle Camonica”, financed through law  
503 77/2006 (financial year 2015) to the Direzione Regionale Musei della Lombardia by the Italian  
504 Ministry of Cultural Heritage and Activities and Tourism. The authors are grateful to Emanuela  
505 Daffra (Director of the Direzione Regionale Musei della Lombardia), Gian Claudio Vaira and all  
506 the personnel of the Rock Engravings National Park of Naquane for logistic assistance during the  
507 field work, to the restorers Alessandro Danesi and Antonella Sechi for the biocide application, and  
508 to Paolo Giordani (University of Genova) for the critical reading of the manuscript. A panel with  
509 the description of the experimental activities was set near Rocks 31 and 30 since 2018 to illustrate

510 the work in progress to the visitors of the Rock Engravings National Park. In this way the  
511 community is made aware of the management efforts for the conservation of the heritage site  
512 inscribed in the WHL and the environment.

513

## 514 **7. References**

515 Arup, U., Søchting, U., Frödén, P., 2013. A new taxonomy of the family Teloschistaceae. Nord. J.  
516 Bot. 31, 016-083. <https://doi.org/10.1111/j.1756-1051.2013.00062.x>

517 Ascaso, C., Wierzchos, J., Souza-Egipsy, V., De los Ríos, A., Rodrigues, J.D., 2002. In situ  
518 evaluation of the biodeteriorating action of microorganisms and the effects of biocides on  
519 carbonate rock of the Jeronimos Monastery (Lisbon). Int. Biodeter. Biodegr. 49, 1-12.  
520 [https://doi.org/10.1016/S0964-8305\(01\)00097-X](https://doi.org/10.1016/S0964-8305(01)00097-X).

521 Baruffo, L., Tretiach, M., 2007. Seasonal variations of  $F_0$ ,  $F_m$ , and  $F_v/F_m$  in an epiphytic population  
522 of the lichen *Punctelia subrudecta* (Nyl.) Krog. Lichenologist 39, 555-565. [https://doi.org/](https://doi.org/10.1017/S0024282907006846)  
523 [10.1017/S0024282907006846](https://doi.org/10.1017/S0024282907006846).

524 Bertuzzi, S., Candotto Carniel, F., Pipan, G., Tretiach, M., 2013. Devitalization of poikilohydric  
525 lithobionts of open-air monuments by heat shock treatments: A new case study centred on  
526 bryophytes. Int. Biodeter. Biodegr. 84, 44-53. <https://doi.org/10.1016/j.ibiod.2013.04.017>.

527 Bertuzzi, S., Gustavs, L., Pandolfini, G., Tretiach, M., 2017. Heat shock treatments for the control  
528 of lithobionts: A case study with epilithic green microalgae. Int. Biodeter. Biodegr. 123, 236-243.  
529 <https://doi.org/10.1016/j.ibiod.2017.06.023>.

530 Brack, P., Dal Piaz, G.V., Baroni, C., Carton, A., Nardin, M., Pellegrini, G.B., Pennacchioni, G.,  
531 2008. Note illustrative della Carta Geologica d'Italia alla scala 1: 50.000. Foglio 058, Monte  
532 Adamello. Carta Geologica d'Italia alla scala 1: 50.000. ISPRA, Roma.

533 Cappitelli, F., Cattò, C., Villa, F., 2020. The control of Cultural Heritage microbial deterioration.  
534 Microorganisms, 8, 1542. <https://doi.org/10.3390/microorganisms8101542>.

535 Cuzman, O., Olmi, R., Riminesi, C., Tiano, P., 2013. Preliminary study on controlling black fungi  
536 dwelling on stone monuments by using a microwave heating system. Int. J. Cons. Sci. 4, 133-144.

537 Darvill, T., Batarda Fernandes, A.P., 2014. Open-air rock-art conservation and management: state  
538 of the art and future perspectives. Routledge, New York.

539 De Cruz, A., Andreotti, A., Ceccarini, A., Colombini, M.P., 2014. Laser cleaning of works of art:  
540 evaluation of the thermal stress induced by Er: YAG laser. Appl. Phys. B 117, 533-541.  
541 <https://doi.org/10.1007/s00340-014-5865-3>.

542 de los Ríos A, Pérez-Ortega S, Wierzchos J, Ascaso C, 2012. Differential effects of biocide  
543 treatments on saxicolous communities: case study of the Segovia cathedral cloister (Spain). Int.  
544 Biodeter. Biodegr. 67, 64-72. <https://doi.org/10.1016/j.ibiod.2011.10.010>.

- 545 Denyer, S. P., Stewart, G.S.A.B., 1998. Mechanisms of action of disinfectants. *Int. Biodeter.*  
546 *Biodegr.* 41, 261-268. [https://doi.org/10.1016/S0964-8305\(98\)00023-7](https://doi.org/10.1016/S0964-8305(98)00023-7).
- 547 Favero-Longo S.E., Benesperi R., Bertuzzi S., Bianchi E., Buffa G., Giordani P., Loppi S.,  
548 Malaspina P., Matteucci E., Paoli L., Ravera S., Roccardi A., Segimiro A., Vannini A., 2017.  
549 Species- and site-specific efficacy of commercial biocides and application solvents against  
550 lichens. *Int. Biodeter. Biodegr.* 123, 127-137. <https://doi.org/10.1016/j.ibiod.2017.06.009>.
- 551 Favero-Longo S.E., Matteucci E., 2022. Indagini diagnostiche sui fenomeni di biodeterioramento e  
552 valutazione sperimentale di strategie per il loro controllo. In: Ruggiero M.G. et al. (Ed.) *Il*  
553 *Progetto “Monitoraggio e buone pratiche di tutela del patrimonio del sito UNESCO n.94 Arte*  
554 *rupestre della Valle Camonica: nuove aree, monoliti dell’età del Rame e pitture” Legge 20*  
555 *febbraio 2006, n.77, E.F. 2015. In press.*
- 556 Favero-Longo S.E., Vannini A., Benesperi R., Bianchi E., Fačkovcová Z., Giordani P., Malaspina  
557 P., Martire L., Matteucci E., Paoli L., Ravera S., Roccardi A., Tonon C., Loppi S., 2020. The  
558 application protocol impacts the effectiveness of biocides against lichens. *Int. Biodet. Biodeg.*,  
559 155, 105105, [doi.org/10.1016/j.ibiod.2020.105105](https://doi.org/10.1016/j.ibiod.2020.105105)
- 560 Favero-Longo S.F., Viles H., 2020. A review of the nature, role and control of lithobionts on stone  
561 cultural heritage: weighing-up and managing biodeterioration and bioprotection. *W. J. Microb.*  
562 *Biot.* 36, 1-18. <https://doi.org/10.1007/s11274-020-02878-3>.
- 563 Gao, K., Yu, H., Brown, M.T., 2007. Solar PAR and UV radiation affects the physiology and  
564 morphology of the cyanobacterium *Anabaena* sp. PCC 7120. *J. Photochem. Photobiol. B:*  
565 *Biology*, 89, 117-124. <https://doi.org/10.1016/j.jphotobiol.2007.09.006>
- 566 Gerosa, G., Finco, A., Oliveri, S., Marzuoli, R., Ducoli, A., Sangalli, G., Comini, B., Nastasio, P.,  
567 Cocca, G., Gagliuzzi, E., 2013. Case Study: Valle Camonica and the Adamello Park, in: Cerbu  
568 G.A., Hanewink, M., Gerosa, G., Jandl, R. (Eds.), *Management strategies to adapt alpine space*  
569 *forests to climate change risks. IntechOpen, Rijeka, pp. 323-354. <http://dx.doi.org/10.5772/56285>.*
- 570 Jensen, M., 2002. Measurement of chlorophyll fluorescence in lichens, in: Kranner, I., Beckett,  
571 R.P., Varma, A.K. (Eds.), *Protocols in lichenology. Springer, Berlin, pp. 135-151.*
- 572 Kalaji, H.M., Jajoo, A., Oukarroum, A., Brestic, M., Zivcak, M., Samborska, I.A., Cetner M.D.,  
573 Łukasik I., Goltsev V. Ladle, R.J., 2016. Chlorophyll a fluorescence as a tool to monitor  
574 physiological status of plants under abiotic stress conditions. *Acta Physiol. Plant.* 38, 102.  
575 <https://doi.org/10.1007/s11738-016-2113-y>.
- 576 Kim, M., Weigand, M. R., Oh, S., Hatt, J.K., Krishnan, R., Tezel, U., Pavlostathis S.G.,  
577 Konstantinidis, K.T., 2018. Widely used benzalkonium chloride disinfectants can promote  
578 antibiotic resistance. *Appl. Environ. Microb.* 84, e01201-18. [https://doi.org/10.1128/AEM.01201-](https://doi.org/10.1128/AEM.01201-18)  
579 [18.](https://doi.org/10.1128/AEM.01201-18)
- 580 Knight, K.B., St. Clair, L.L., Gardner, J.S., 2004. Lichen biodeterioration at inscription rock, El  
581 Morro national monument, Ramah, New Mexico, USA, in: Seaward, M.R.D., St. Clair, L.L.  
582 (Eds.), *Biodeterioration of stone surfaces. Springer, Dordrecht, pp. 129-163.*



- 583 Kvíderová, J., Kumar, D., 2020. Response of short-term heat shock on photosynthetic activity of  
584 soil crust cyanobacteria. *Protoplasma* 257, 61-73. <https://doi.org/10.1007/s00709-019-01418-7>.
- 585 Lalley, J.S., Viles, H.A., 2006. Do vehicle track disturbances affect the productivity of soil-growing  
586 lichens in a fog desert? *Funct. Ecol.* 20, 548-556. <https://doi.org/10.1111/j.1365-2435.2006.01111.x>.
- 588 Lange, O.L., 1953. Hitze-und Trockenresistenz der Flechten in Beziehung zu ihrer Verbreitung.  
589 *Flora oder Allgemeine Botanische Zeitung* 140, 39-97. [https://doi.org/10.1016/S0367-1615\(17\)31917-1](https://doi.org/10.1016/S0367-1615(17)31917-1).
- 591 Macana, R.J., Baik, O.D., 2018. Disinfestation of insect pests in stored agricultural materials using  
592 microwave and radio frequency heating: A review. *Food Rev. Int.*, 34, 483-510.  
593 <https://doi.org/10.1080/87559129.2017.1359840>.
- 594 MacFarlane, J.D., Kershaw, K.A., 1980. Physiological-environmental interactions in lichens: IX.  
595 thermal stress and lichen ecology. *New Phytol.* 84, 669-685. <https://doi.org/10.1111/j.1469-8137.1980.tb04780.x>.
- 597 Malaspina, P., Giordani, P., Pastorino, G., Modenesi, P., Mariotti, M.G. 2015. Interaction of sea salt  
598 and atmospheric pollution alters the OJIP fluorescence transient in the lichen *Pseudevernia*  
599 *furfuracea* (L.) Zopf. *Ecol. Indic.* 50, 251-257. <https://doi.org/10.1016/j.ecolind.2014.11.015>.
- 600 Marečková, M., Barták, M., Hájek, J., 2019. Temperature effects on photosynthetic performance of  
601 Antarctic lichen *Dermatocarpon polyphyllizum*: a chlorophyll fluorescence study. *Polar Biol.* 42,  
602 685-701. <https://doi.org/10.1007/s00300-019-02464-w>.
- 603 Martin-Sanchez, P. M., Nováková, A., Bastian, F., Alabouvette, C., Saiz-Jimenez, C., 2012. Use of  
604 biocides for the control of fungal outbreaks in subterranean environments: the case of the Lascaux  
605 Cave in France. *Environ. Sci. Technol.*, 46, 3762-3770. <https://doi.org/10.1021/es2040625>
- 606 Mascalchi, M., Osticioli, I., Riminesi, C., Cuzman, O.A., Salvadori, B., Siano, S. 2015. Preliminary  
607 investigation of combined laser and microwave treatment for stone biodeterioration. *Stud.*  
608 *Conserv.* 60(Suppl. 1), 19-26. <https://doi.org/10.1179/0039363015Z.000000000203>.
- 609 Mascalchi, M., Orsini, C., Pinna, D., Salvadori, B., Siano, S., Riminesi, C., 2020. Assessment of  
610 different methods for the removal of biofilms and lichens on gravestones of the English Cemetery  
611 in Florence. *Int. Biodeter. Biodegr.*, 154, 105041. [doi.org/10.1016/j.ibiod.2020.105041](https://doi.org/10.1016/j.ibiod.2020.105041).
- 612 Matteucci E., Scarcella A.V., Croveri P., Marengo A., Borghi A., Benelli C., Hamdan O., Favero-  
613 Longo S.E., 2019. Lichens and other lithobionts on the carbonate rock surfaces of the heritage site  
614 of the tomb of Lazarus (Palestinian territories): diversity, biodeterioration, and control issues in a  
615 semi-arid environment. *Ann. Microbiol.* 69, 1033-1046. <https://doi.org/10.1007/s13213-019-01465-8>.
- 617 Metaxas A.C., Meredith, R.J., 2011. *Industrial Microwave Heating*. The Institution of Engineering  
618 and Technology, London.

- 619 Nayaka, S., Ranjan, S., Saxena, P., Pathre, U.V., Upreti, D.K., Singh, R., 2009. Assessing the  
620 vitality of Himalayan lichens by measuring their photosynthetic performances using chlorophyll  
621 fluorescence technique. *Curr. Sci.* 97, 538-545.
- 622 Pinna, D., 2017. Coping with biological growth on stone heritage objects: Methods, products,  
623 applications, and perspectives. CRC Press, Boca Raton.
- 624 Pozo-Antonio, J.S., Barreiro, P., González, P., Paz-Bermúdez, G., 2019. Nd: YAG and Er: YAG  
625 laser cleaning to remove *Circinaria hoffmanniana* (Lichenes, Ascomycota) from schist located in  
626 the Côa Valley Archaeological Park. *Int. Biodeter. Biodegr.* 144: 104748.  
627 <https://doi.org/10.1016/j.ibiod.2019.104748>.
- 628 Pozo-Antonio, J. S., Sanmartín, P., 2018. Exposure to artificial daylight or UV irradiation (A, B or  
629 C) prior to chemical cleaning: an effective combination for removing phototrophs from granite.  
630 *Biofouling* 34, 851-869. <https://doi.org/10.1080/08927014.2018.1512103>.
- 631 Riminesi, C., Olmi, R., 2016. Localized microwave heating for controlling biodeteriogens on  
632 cultural heritage assets. *Int. J. Cons. Sci.* 7(Special Issue 1), 281-294.
- 633 Sanmartín, P., Fuentes, E., Montojo, C., Barreiro, P., Paz-Bermúdez, G., Prieto, B., 2019. Tertiary  
634 bioreceptivity of schists from prehistoric rock art sites in the Côa Valley (Portugal) and Siega  
635 Verde (Spain) archaeological parks: Effects of cleaning treatments. *Int. Biodeter. Biodegr.* 142,  
636 151-159. <https://doi.org/10.1016/j.ibiod.2019.05.011>.
- 637 Sanmartín, P., Rodríguez, A., Aguiar, U., 2020. Medium-term field evaluation of several widely  
638 used cleaning-restoration techniques applied to algal biofilm formed on a granite-built historical  
639 monument. *Int. Biodeter. Biodegr.* 147, 104870. <https://doi.org/10.1016/j.ibiod.2019.104870>.
- 640 Sanmartín, P., Villa, F., Polo, A., Silva, B., Prieto, B., Cappitelli, F., 2015. Rapid evaluation of  
641 three biocide treatments against the cyanobacterium *Nostoc* sp. PCC 9104 by color changes. *Ann.*  
642 *Microbiol.* 65, 1153-1158. <https://doi.org/10.1007/s13213-014-0882-3>.
- 643 Sanz, M., Oujja, M., Ascaso, C., de los Ríos, A., Pérez-Ortega, S., Souza-Egipsy, V., Wierzchos, J.,  
644 Speranza, M., Vega Cañamares, M., Castillejo, M., 2015. Infrared and ultraviolet laser removal of  
645 crustose lichens on dolomite heritage stone. *Appl. Surf. Sci.* 346, 248–255.  
646 <https://doi.org/10.1016/j.apsusc.2015.04.013>.
- 647 Scheerer, S., Ortega-Morales, O., Gaylarde, C., 2009. Microbial deterioration of stone  
648 monuments—an updated overview. *Adv. Appl. Microbiol.*, 66, 97-139.  
649 [https://doi.org/10.1016/S0065-2164\(08\)00805-8](https://doi.org/10.1016/S0065-2164(08)00805-8).
- 650 Soni, A., Smith, J., Thompson, A., Brightwell, G., 2020. Microwave-induced thermal sterilization-  
651 A review on history, technical progress, advantages and challenges as compared to the  
652 conventional methods. *Trends Food Sci. Technol.* 97, 433-442.  
653 <https://doi.org/10.1016/j.tifs.2020.01.030>.
- 654 Stirbet, A., Govindjee S.A., 2011. On the relation between the Kautsky effect (chlorophyll a  
655 fluorescence induction) and photosystem II: basics and applications of the OJIP fluorescence  
656 transient. *J. Photoch. Photobio. B: Biology* 104, 236-257.  
657 <https://doi.org/10.1016/j.jphotobiol.2010.12.010>.

- 658 Stirbet, A., Lazár, D., Papageorgiou, G.C., 2019. Chlorophyll a fluorescence in cyanobacteria:  
659 relation to photosynthesis, in: Mishra, A.K., Tiwari, D.N., Rai, A.N. (Eds.), *Cyanobacteria: From*  
660 *basic science to applications*. Academic Press, London, pp. 79-130. [https://doi.org/10.1016/B978-](https://doi.org/10.1016/B978-0-12-814667-5.00005-2)  
661 [0-12-814667-5.00005-2](https://doi.org/10.1016/B978-0-12-814667-5.00005-2).
- 662 Strasser, B.J., 1997. Donor side capacity of photosystem II probed by chlorophyll a fluorescence  
663 transients. *Photosynth. Res.* 52, 147-155. <https://doi.org/10.1023/A:1005896029778>.
- 664 Tratebas, A.M., 2004. Biodeterioration of Prehistoric rock art and issues in site preservation, in:  
665 Seaward, M.R.D., St. Clair, L.L. (Eds.), *Biodeterioration of stone surfaces*. Springer, Dordrecht,  
666 pp. 195-228.
- 667 Tretiach, M., Bertuzzi, S., Candotto Carniel, F., 2012. Heat shock treatments: a new safe approach  
668 against lichen growth on outdoor stone surfaces. *Environ. Sci. Technol.* 46, 6851-6859.  
669 <https://doi.org/10.1021/es3006755>.
- 670 Tretiach, M., Bertuzzi, S., Salvadori, O., 2010. Chlorophyll a fluorescence as a practical tool for  
671 checking the effects of biocide treatments on endolithic lichens. *Int. Biodeter. Biodeg.* 64, 452-  
672 460. <https://doi.org/10.1016/j.ibiod.2010.05.004>.
- 673 UNESCO, 2008. List of factors affecting the properties: <https://whc.unesco.org/en/factors/>.  
674 Accessed on 27 July 2020.
- 675 Vivas, M., Pérez-Ortega, S., Pintado, A., Sancho, L.G., 2017.  $F_v/F_m$  acclimation to the  
676 Mediterranean summer drought in two sympatric *Lasallia* species from the Iberian mountains.  
677 *Lichenologist* 49, 157-165. <https://doi.org/10.1017/S0024282917000032>.
- 678 Vondrak, J., Kubásek, J., 2013. Algal stacks and fungal stacks as adaptations to high light in  
679 lichens. *Lichenologist* 45, 115-124. <https://doi.org/10.1017/S0024282912000722>.
- 680 Wessels, S., Ingmer, H., 2013. Modes of action of three disinfectant active substances: a review.  
681 *Regul. Toxicol. Pharm.* 67, 456-467. <https://doi.org/10.1016/j.yrtph.2013.09.006>
- 682 Zhang, L., Liu, J., 2016. Effects of heat stress on photosynthetic electron transport in a marine  
683 cyanobacterium *Arthrospira* sp. *J. Appl. Phycol.* 28, 757-763. [https://doi.org/10.1007/s10811-015-](https://doi.org/10.1007/s10811-015-0615-4)  
684 [0615-4](https://doi.org/10.1007/s10811-015-0615-4).

685 **Figure captions**

686 Fig. 1. Microwave treatment on Rock 30 (Rock Engravings National Park of Naquane, Valle  
687 Camonica, Italy). (a) the portable microwave system; (b) microwave applicator on a parcel (30 × 30  
688 cm) with *Rufoplaca arenaria* (\*); (c) microwave application with an interposed layer of cellulose  
689 poultice; (d-f) a surface with *Xanthoparmelia conspersa* before (T<sub>0M</sub>, d) and 40 days after (T<sub>40M</sub>; e)  
690 the microwave treatment with the applicator in direct contact with the rock, and after the successive  
691 cleaning using mechanical tools (f).

692 Fig. 2. Maximum quantum yield of PSII ( $F_v/F_m$ ) in *Xanthoparmelia conspersa* (a), *Rufoplaca*  
693 *arenaria* (b) and the phototrophic biofilm (c) 4-6 hours before (T<sub>0</sub>) and 24 hours (T<sub>1</sub>) and 40 days  
694 (T<sub>40</sub>) after the treatment with deionized water only (DW), Preventol (PV), Biotin T (BT), Biotin R  
695 (BR), and microwaves (MW), applied directly (brush or direct MW contact; light box plots) or with  
696 the cellulose poultice (dark box plots). For each case study (biocidal approach × application method  
697 × species), box plots not sharing any capital letter (A, B, C) differ significantly ( $P < 0.05$ ).  $F_v/F_m$   
698 values that significantly decreased below the threshold fixed at 0.15 ( $P < 0.05$ ), indicative of  
699 devitalization, are marked (\*).

700 Fig. 3.  $F_0$  values *Xanthoparmelia conspersa* (a), *Rufoplaca arenaria* (b) and the phototrophic  
701 biofilm (c) 4-6 hours before (T<sub>0</sub>) and 24 hours (T<sub>1</sub>) and 40 days (T<sub>40</sub>) after the treatment with  
702 deionized water only (DW), PV, BT, BR, and MW, applied directly (brush or direct MW contact;  
703 light columns) or with the cellulose poultice (dark columns). For each case study (biocidal approach  
704 × application method × species), box plots not sharing any capital letter (A, B, C) differ  
705 significantly ( $P < 0.05$ ).  $F_0$  values that decreased at T<sub>1</sub> and T<sub>40</sub> more than 80% with respect to T<sub>0</sub>  
706 ( $P < 0.05$ ) are marked (\*).

707 Fig. 4. OJIP transients of *Xanthoparmelia conspersa* (a), *Rufoplaca arenaria* (b) and the  
708 phototrophic biofilm (c) before (T<sub>0M</sub>, filled quadrats), and 24 hours (T<sub>1M</sub>, crossed quadrats) and 40  
709 days (T<sub>40M</sub>, empty quadrats) after microwave radiation applied directly (black symbols) or with an  
710 interposed layer of cellulose poultice (red symbols). Time is expressed as seconds; fluorescence is  
711 expressed as arbitrary units.

712 Fig. 5. Real-time temperature monitoring of surfaces treated with microwaves. (a) times ( $av \pm SD$ )  
713 needed to reach temperature thresholds (from 30° to 80°C) after the beginning of microwave  
714 application; (b) time intervals ( $av. \pm SD$ ) in which the rock surfaces colonized by *Xanthoparmelia*  
715 *conspersa* (X), *Rufoplaca arenaria* (R) and the phototrophic biofilm (P) were exposed to  
716 temperatures higher than thresholds ranging from 30°C to 80°C. The treatment was carried out with  
717 the microwave applicator positioned directly on the rock surface (black symbols, a, black columns,  
718 b) or with an interposed layer of cellulose poultice (red symbols, a; red columns, b). For each  
719 temperature threshold, couples of points marked with an asterisk (a) and columns not sharing any  
720 capital letter (b) significantly differ ( $P < 0.05$ ).

721

722 Table 1. Synoptic comparison of the treatment effectiveness against the foliose lichen  
 723 *Xanthoparmelia conspersa*, the crustose lichen *Rufoplaca arenaria* and the cyanobacterial  
 724 phototrophic biofilm, evaluated after the application of biocides (Preventol, PV; Biotin T, BT;  
 725 Biotin R, BR) and microwaves (MW) (at T40 with respect to T0).

	Foliose lichen	Crustose lichen	Photo-trophic biofilm	Foliose lichen	Crustose lichen	Photo-trophic biofilm
	Application by brush			Application with cellulose poultice		
PV	-	-	†	†*	-	†*
BT	-	=	†	†*	†	†
BR	-	=	=	†*	†*	†*
	Direct application			Interposed cellulose poultice		
MW	†*	†*	†*	†*	-	†

726 =, no significant decrease of  $F_v/F_m$ , and  $F_0$  decrease lower than -80%

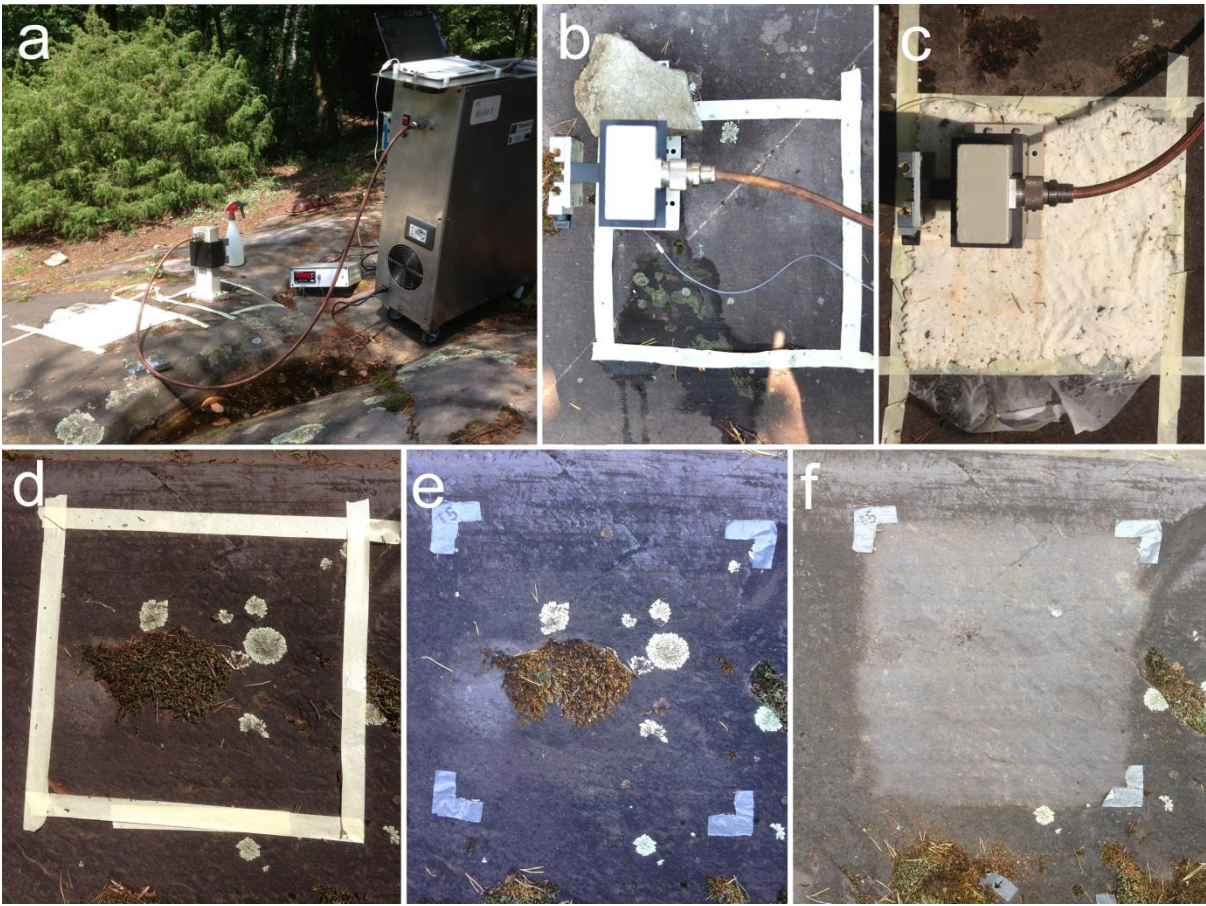
727 -, significant decrease of  $F_v/F_m$ , but not below the 0.15 threshold, and  $F_0$  decrease lower than -80%

728 †, significant decrease of  $F_v/F_m$ , but not below the 0.15 threshold, and  $F_0$  decrease higher than -80%

729 †\*, significant decrease of  $F_v/F_m$  below 0.15, and  $F_0$  decrease higher than -80%

730

731



732

